Neural Mechanisms underlying the Switch from Freeze to Action

The role of defensive reactions in emotional action selection

by

Manon Maarseveen

Supervised by:

    1. Dr. B.P. Bramson (Bob)

    2. Prof. Dr. K. Roelofs (Karin) - PI

    3. Dr. R.C.G. Helmich (Rick)   - 2nd reader

Radboud University Nijmegen

Date of final oral examination: July 13, 2021

Manon Maarseveen
S4764552

Abstract

Defensive freezing is characterized by postural immobility and heart rate deceleration (bradycardia), and has been linked to action preparation. Although subregions of the medial cingulate cortex (MCC) and anterior cingulate cortex (ACC) are activated during freeze and the switch to action, respectively, it remains unclear whether and how they communicate with the sensorimotor cortex (SMC). To examine the neural mechanisms underlying freeze and the subsequent switch to action, we applied magnetoencephalography (MEG) during an active shooting task, in which participants prepared and performed actions under the threat of shock. Threat anticipatory freezing was indicated by more severe heart rate deceleration under the threat of shock versus safety. Importantly, decreased alpha- and beta-band rhythmic activity was shown during action preparation under threat of shock. Finally, the ACC is suggested to be related to the switch from freeze to action, which is associated with a release from MCC to SMC inhibition. Taken together, the results confirm that freezing can be seen as an active state that relates to action preparation. However, we could only include the first half (N = 24) of the target number of participants in the analysis. Therefore, future investigations including a powerful sample size are needed to obtain a more reliable overview of the electrophysiological mechanisms underlying the switch from freeze to action.

Keywords: Freezing, Action Preparation, Switch to Action, MEG, Anterior/Medial Cingulate Cortex, Sensorimotor Cortex

1. Introduction

Imagine you are on the tram on your way to university when all of a sudden one of the fellow travellers pulls out a gun. It is very likely that this will frighten you and that you will freeze. In order to survive, it is often necessary to switch to an action to avoid the danger. For instance, when such an attack took place in Utrecht in 2019, most of the survivors were able to override the freeze response to flee from the tram. This example highlights that it is vital to quickly switch from the initial freezing response to an active defensive response such as fleeing or fighting.

The current study focuses on how the switch from freeze to action is implemented in the brain. Revealing these neural mechanisms is relevant for humans in high-risk professions (e.g., police officers) who have to perform optimally under stress. To illustrate, despite good training to deal with threat, these professionals appear to have difficulties in controlling their actions in stressful situations (Roelofs, 2017).

Previous research has shown that defensive freezing is characterized by heart rate deceleration (bradycardia) and reduced body movements (Roelofs, Hagenaars & Stins, 2010; Hagenaars, Oitzl & Roelofs, 2014). During freeze, one is extremely sensitive to environmental cues that enable optimal detection of danger and prime active defensive behaviours (Lojowska, Mulckhuyse, Hermans & Roelofs, 2019; Roelofs et al., 2010). This response is evolutionary advantageous since it reduces the chance of being detected by a predator, while it promotes the preparation for active fight-or-flight responses (Hagenaars et al., 2014; Lojowska, Gladwin, Hermans & Roelofs, 2015). Recently, freezing is increasingly seen as an active preparatory state during which restraining processes and action preparation occur simultaneously (Gladwin, Hashemi, van Ast & Roelofs, 2016; Hashemi et al., 2019a). This view is supported by the idea that freezing is accompanied by synchronous activity in the sympathetic and parasympathetic branches of the autonomic nervous system (Hagenaars et al., 2014; Lojowska, Ling, Roelofs & Hermans, 2018; Roelofs, 2017).

At the neural level, it has been shown that freezing is accompanied by activity in the anterior medial cingulate cortex (aMCC; Hashemi et al., 2019a). Similar findings were shown in rodent studies, where activity in the medial prefrontal cortex (mPFC) was linked to controlling threat-related motor behaviour and autonomic nervous system activity (Grunfeld & Likhtik, 2018; Karalis et al., 2016). Moreover, when there is a possibility to act in order to avoid the threat, freezing also elicited activity in the sensorimotor cortex (SMC), which is suggested to reflect action preparation (Hashemi et al., 2019a). Furthermore, in rodents, it has been indicated that freezing is accompanied by increased synchronized neuronal activity in the theta-band (4-12 Hz; Stujenske, Likhtik, Topiwala & Gordon, 2014; Karalis et al., 2016; Rozeske & Herry, 2018). Specifically, the aMCC seems to be involved in the generation of low-frequency fear-evoked theta rhythms (4-6 Hz; Grunfeld & Likhtik, 2018).

When switching to an action, there is a reduction in parasympathetic activity, which is accompanied by activity in the pregenual anterior cingulate cortex (pACC; Roelofs, 2017; Lojowska et al., 2018; Hashemi et al., 2019a). These results are supported by recent rodent work that highlighted that the pACC causes a decrease in the freezing response, whereas the aMCC is indeed involved in the expression of defensive freezing (Grunfeld & Likhtik, 2018).

Taken together, earlier work suggested that freezing can be seen as an active state that is related to action preparation. Here, subregions of the MCC are involved during threat-anticipation, whereas subareas of the ACC appear to take over during the switch to action. However, it is not yet established how the switch from freeze to action is neurally implemented in humans. Hence, the aim of this study was to unravel the electrophysiological mechanisms of freezing in relation to action preparation and the subsequent switch to action. To investigate this, participants had to perform a shooting task while magnetoencephalography (MEG) was recorded. During the task, participants competed against virtual opponents that either held up a gun or a phone. Depending on which object the opponent drew, quick decisions had to be made on whether to shoot or withhold a response. Here, threat was manipulated by receiving an electrical shock following erroneous responses.

On the neural level, we expected that theta-band rhythmic activity increased in the MCC during threat anticipation to maintain freeze. Furthermore, we hypothesised that the switch from freezing to action is reflected in a shift from MCC to ACC activity (Grunfeld & Likhtik, 2018). As a result, the SMC will be released from MCC inhibition, which might be reflected by decreases in alpha-band (8-12 Hz) and beta-band (15-25 Hz) rhythmic activity (Grunfeld & Likhtik, 2018; Jensen & Mazaheri, 2010; Stolk et al., 2019).

2. Materials & Methods

2.1 Participants

Twenty-six healthy participants (13 females, 19-33 years, mean age 23.8 years) were recruited from the Radboud University participant pool to participate in exchange for monetary compensation. Two participants were excluded from analysis due to poor task performance (n=1) and discontinuation of the experiment (n = 1). Participants were right-handed or ambidextrous, had normal or corrected-to-normal vision, and reported no history of neurological illness. Prior to the experiment, all participants signed the study specific informed consent in accordance with the guidelines of the local ethical committee (CMO2014/288).

2.2 Experimental task

For the current study, participants performed a shooting task during which action preparation under the threat of shock was measured (see Figure 1; Gladwin et al., 2016; Hashemi et al., 2019a,b). The experiment was generated with Presentation (Version: 20.2 07.25.18), and contained a practice block and eight experimental blocks consisting of twenty trials.

At the start of a trial, participants viewed a parking garage where one of two randomly presented virtual opponents appeared. The opponent could perform two actions: they either drew a gun (Go stimulus) or held up a mobile phone (No-Go stimulus) towards the participant. Following this, participants could prepare an action during a long (7000-9000 ms; 80%), middle (5000-7000 ms; 10%), or short (1000-3000 ms; 10%) cue-stimulus interval (CSI). Most trials consisted of long preparation intervals, which were needed to determine the time course of heart rate deceleration during threat anticipation. Shorter trials were included to make the moment of action unpredictable.

The preparation interval was followed by a response window (individually titrated, starting at 550 ms), which will be further referred to as the draw. During the draw, participants had to fire their gun if the opponent pulled out a gun, and they had to withhold their response when a phone was held up. Participants could shoot the opponent by pressing a button. When the participant made an erroneous response, or responded too late, the participant was being shot virtually. For one opponent (threat trial), being shot was associated with an electrical shock that was set to an uncomfortable but not painful level using a standardized work-up procedure (Klumpers et al., 2010). For the other opponent (safe trial), being shot was never associated with an electrical shock, and the participants only received visual feedback after their responses. Which of the opponents was representative of threat trials was randomised among participants. Every trial was followed by a variable inter-trial interval (ITI, 5000 – 9000 ms).

To keep the number of received electrical shocks consistent across blocks and between participants, the length of the response window was adjusted after every trial. This titration was based participants' performance on previous trials, meaning that the time to respond to next trials decreased by 10% after every correct response, whereas it increased after a mistake has been made. This titration procedure ensured that participants were shot in ~50% of the trials.
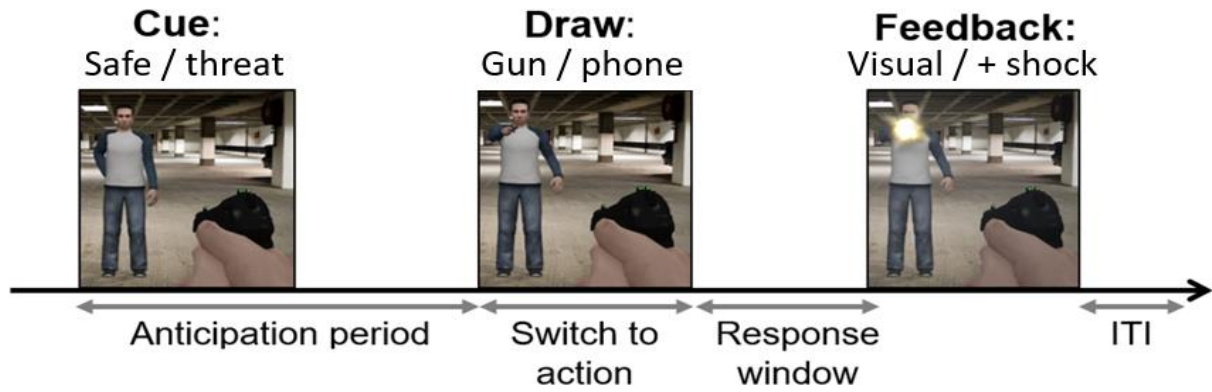
Figure 1: Illustration of the shooting task.

One of two avatars appears on the screen, for one there is a risk of shock (threat trials), for the other one not (safe trials). Participants have to shoot the opponent as fast as possible if a gun is drawn, but hold their fire if a phone is pulled. An erroneous response will result in a shock (threat trials only).

2.3 MEG data acquisition

Participants were positioned in the MEG helmet, 80 cm from a screen where the shooting task was presented using a PROPixx beamer (resolution: 1920x1080; refresh rate: 120 Hz). MEG data was obtained using a whole-brain CTF-275 system with axial gradiometers. Six SQUID sensors were permanently disabled due to high noise levels (MRF66, MLC11, MCL32, MLO33, MRO33, MLC61). The signals were recorded at a sampling rate of 1200 Hz. Head localization coils were placed on the nasion and in both ears. During the experiment, head location was continuously measured using online head localization software (Stolk, Todorovic, Schoffelen & Oostenveld, 2013). In this way, head movements could be kept as low as possible (maximum movements were ~5 mm). Participants' eye movements and pupil area were monitored using an EyeLink 1000 eyetracker, sampled at 1000 Hz. Reponses were made by a button press on a Fiber optic response pad. After erroneous responses on threat trials, participants received an electrical stimulation on the left index finger generated by a Digitimer Constant Current Stimulator (model DS7A).

2.4 Behavioural analysis

The behavioural performance of the participants was analysed by assessing the mean accuracy and reaction time per condition. As for the latter, trials in which the response times exceeded three standard deviations of the mean (calculated per participant) were excluded from further analysis. Next, mean accuracy was compared between the different threat conditions (threat or safe) and armed conditions (gun or phone), by conducting a two-way repeated measures ANOVA. Mean reaction time was calculated on correct shoot trials only, for which the performance on threat and safe trials was compared using a paired samples t-test. All statistical analyses regarding participants' behavioural performance were conducted in R (https://www.r-project.org/).

2.5 Heart rate analysis

Using independent component analysis (ICA), the heart rate was extracted from the raw MEG data. Only trials with a preparation interval of at least six seconds were included in the analysis to be able to calculate threat-related bradycardia (see Gladwin et al., 2016; Hashemi et al., 2019b). The data of two participants were excluded because the cue stimulus intervals were shorter, resulting in too few trials of the required length. For every trial, the time points of heart rate peaks were registered based on which the heart rate in beats per minute (BPM) could be calculated. Trials where the peaks were not clearly detectable were removed from further analysis. Heart rate changes were assessed from stimulus onset until the moment the opponent drew a gun or phone, and were baseline-corrected by subtracting the mean heart rate during the last second before stimulus onset. To compute heart rate differences between threat and safe trials, mean heart rate change was calculated for nine time points during the preparation interval. These time points reflected the mean heart rate during a 500 ms time window that was centered at 3.0 s, 3.5 s, 4.0 s, 4.5 s, 5.0 s, 5.5 s, 6.0 s, 6.5 s and 7.0 s (see Hashemi et al., 2019a). Subsequently, a repeated-measures ANOVA was conducted with the nine time points and threat condition (threat or safe) as within-subject variables. Additionally, to analyse the effects of threat condition and heart rate changes on reaction time, a linear mixed-effects model was fit with heart rate, threat condition and their interaction as fixed effects, and with random intercepts and random slopes per subject for all three fixed effects. Here, the heart rate change after six seconds (relative to baseline) was taken as predictor. Furthermore, p-values were computed using Kenward-Roger approximation of degrees of freedom.

2.6 MEG analysis

All MEG data analyses were conducted in MATLAB (version 2018b) using the open source toolbox FieldTrip (Oostenveld, Fries, Maris & Schoffelen, 2011) and custom-written scripts. To start MEG data preprocessing, the data was first epoched into trials, including 2000 ms before stimulus onset and after the draw. Subsequently, the data was demeaned, linear trends were extracted and line noise was removed using the discrete Fourier transform. On trials where a shock was delivered, the shock artifact was removed and the missing data frame with a length of 10 ms was linearly interpolated based on the surrounding data values (10 ms before and after the interpolation window). Next, the variances in the data were visually inspected, after which trials and channels with extreme values were excluded from further analysis. Finally, the data was resampled to 150 Hz and ICA was performed to remove ocular and heart artifacts.

Using the preprocessed data, virtual channels were created for the sources of interest: the medial cingulate cortex (MCC), anterior cingulate cortex (ACC) and sensorimotor cortex (SMC). To achieve this, a single-shell head model and source model were computed for each participant using an anatomical MRI and Polhemus head shape digitization. Subsequently, an independent spatial filter was created using linearly constrained minimum variance (LCMV) beamforming without applying time-domain filters (Van Veen, Van Drongelen, Yuchtman & Suzuki, 1997). Using a multimodal parcellation atlas (Glasser et al., 2016), source-level time series could be extracted for MCC, ACC and SMC independently (see Supplementary Materials S1). The resulting virtual channels were used to perform frequency and connectivity analyses.

For the main study, MEG analyses were performed on the data of all participants that had been included so far. Additionally, the analyses were repeated only including participants who showed threat-related bradycardia (see Supplementary Materials S2).

2.6.1 Power spectral density

During the preparation window, the power of each frequency was revealed by conducting a power spectral density (PSD) analysis. Trials with a preparation interval of at least six seconds were included in this analysis and subsequent analyses. To increase power, the trial-level data was chunked into one-second segments. Power spectral density was computed between 0 and 100 Hz by means of the fast Fourier transform including a Hanning taper. The frequency content of the signal was determined for both the threat and safe condition, and was independently calculated for the MCC, ACC and SMC.

2.6.2 Time-frequency representation

The electrophysiological changes underlying the switch from freeze to action were investigated by calculating time-frequency representations (TFRs) of power. Here, the time window of the analysis included half a second before and one second after the moment the opponent performed an action. To avoid that the analyses were affected by the delivered shocks, whilst keeping the number of trials in the threat and safe condition approximately equal, trials containing incorrect responses were removed. Time-frequency analyses were calculated between 0 and 40 Hz as well as between 40 and 150 Hz, using a sliding window Hanning taper based approach and a multitaper based approach, respectively. For the first analysis, the spectral resolution was 2 Hz, and a time window with a fixed length of 500 ms was moved over the signal in steps of 50 ms. To analyse frequencies above 40 Hz, the spectral resolution was set to 5 Hz, and the time window was slid over the data in steps of 1 ms. Here, we used a frequency-dependent window to ensure that each time window contained 6 cycles of the respective frequency. Furthermore, the amount of spectral smoothing was set to 40%, which made it increase with frequency. We calculated the results for the MCC, ACC and SMC independently, and relative power differences between the conditions were visualised. The data of four participants were excluded due to recording artifacts that disrupted the signal during the draw.

2.6.3 Connectivity

Connectivity analyses were performed to reveal patterns of synchronous activation between MCC, ACC and SMC, during both the anticipation window (stimulus onset to six seconds after) and the draw (stimulus onset to one second after). Again, the trial-level data involving the anticipation window was chunked into one-second segments to increase power. First, synchrony in neural activity between the brain regions was determined by calculating the coherence spectra (Fries, 2005). To achieve this, the cross-spectral density matrix was computed by calculating the Fourier representation of the signal (from 0 to 150 Hz, using multitapers), after which the spectral representation of one signal was multiplied with the complex conjugate of the spectral representation of the other signal (Bastos & Schoffelen, 2016). Second, to see if there is any directional connectivity from MCC to SMC during the anticipation window, and from ACC to SMC during the switch to action, Granger

causality was calculated. For this analysis, the cross-spectral density matrix was generated in a non-parametric way by applying Fourier decomposition using multitapers. Thereafter, the spectral transfer function could be calculated using spectral factorisation of the cross-spectral density matrix (Bastos & Schoffelen, 2016).

2.6.4 Statistical analysis

At the group level, the conditions were statistically compared by performing cluster-based permutation tests (Maris & Oostenveld, 2007; Maris, 2011). For the power spectral density analysis, threat and safe trials were compared whereby clusters could be formed across the frequency dimension. Concerning the connectivity analyses, clustering could happen across the same dimension, but in addition to the threat-safe comparison during anticipation, it was also examined whether there was a difference during the draw between shoot trials in the threat and safe condition. Furthermore, clusters could be formed in the time-frequency domain for the time-frequency representations. Here, it was investigated whether there was a difference between correct shoot and withhold trials, and also whether a difference could be found between threatening compared to safe shoot trials.

To achieve these analyses, dependent sample t-values were calculated to quantify the respective conditional differences. Only samples with t-values larger than the specified threshold ($\alpha = 0.05$) were selected, and clustered based on spectral or spectro-temporal adjacency. Next, the t-values were summed within a cluster and the maximum of this was taken as cluster-level statistic. Using these values, Monte Carlo significance probability was calculated which included 500 randomisations.

3. Results

3.1 Behavioural results

Mean accuracy was calculated for each threat condition (threat or safe) and armed condition (gun or phone). The percentage of correct trials was highest for safe withhold trials (M = 83.44%, SD = 37.19%), followed by threat withhold trials (M = 79.90%, SD = 40.10%), threat shoot trials (M = 57.71%, SD = 49.43%) and safe shoot trials (M = 47.29%, SD = 49.95%). To see whether participants' accuracy differed significantly across conditions, a two-way repeated measures ANOVA was computed on the mean accuracy. This revealed a significant main effect of threat condition ($F(1,23) = 6.42$, $p = 0.019$) and armed condition ($F(1,23) = 245.27$, $p < 0.0001$), and a significant interaction effect between these factors ($F(1,23) = 9.96$, $p = 0.0044$; see Figure 2A). These results show that participants were overall more accurate on withhold trials compared to shoot trials. Furthermore, participants shot more accurately on threat trials, while they were more accurate on safe trials when they had to withhold their response.

A paired samples t-test was conducted to reveal if response times differed significantly between safe (M = 291.59 ms, SD = 78.90 ms) and threat (M = 274.78 ms, SD = 57.56 ms) trials. The assumptions of normality and equal variances were checked beforehand by performing a Shapiro-Wilk test (threat: $W = 0.97$, $p = 0.63$; safe: $W = 0.96$, $p = 0.38$) and a Levene's test ($F(1,46) = 0.32$, $p = 0.58$), respectively. A significant difference in reaction time was found between the threat conditions ($t(23) = 3.59$, $p = 0.0016$), indicating that participants were faster on threat compared to safe trials (see Figure 2B).
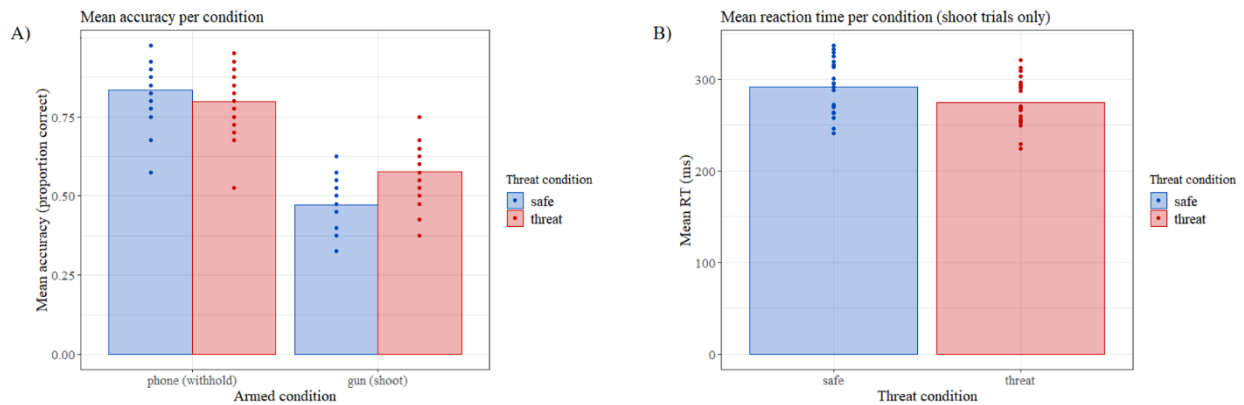

Figure 2: Behavioural results per condition.

Panel A shows the group level mean accuracy per threat condition (safe or threat) and armed condition (gun or phone). The red bars represent the mean group accuracy on threat trials, the blue bars on safe trials. The dots reflect the mean performance per individual. There was a significant effect for threat condition, armed condition and the interaction between these factors. B) Here, the mean reaction time is plotted per threat condition, including shoot trials only. A significant effect of threat condition on reaction time could be observed.

3.2 Heart rate results

Heart rate differences were calculated per threat condition (threat or safe), and were compared by means of a repeated-measures ANOVA. After a Greenhouse-Geisser correction was applied to the degrees of freedom, a significant main effect was observed for the nine time points (between 3.0 and 7.0 s) ($F(1.33,27.84) = 53.61$, $p < 0.0001$), as well as a significant interaction between time points and threat condition ($F(2.60, 54.63) = 5.63$, $p = 0.0030$; see Figure 3). The assumption of sphericity was not violated for the threat condition, but no significant conditional difference was found either. Post-hoc paired samples t-tests were calculated on every time point to compare heart rate changes between safe and threat trials, but this yielded no significant results (e.g., at 6.5 s, p = 0.17). Taken together, the results indicate that during the later parts of anticipation (3.0 to 7.0 s), the heart rate decrease is significantly stronger for threat compared to safe trials.

A linear mixed-effects model was fitted to examine the effects of threat condition and heart rate changes on reaction time. A significant effect of threat condition on reaction time could be shown ($F(20, 68) = 15.01$, $p = 0.0010$), which corresponds to the reaction time results we found earlier, as detailed in the behavioural results section. No other main effects or interaction effects were observed. The mixed model was applied despite a singular fit warning. However, the results hardly changed after applying different optimizers.
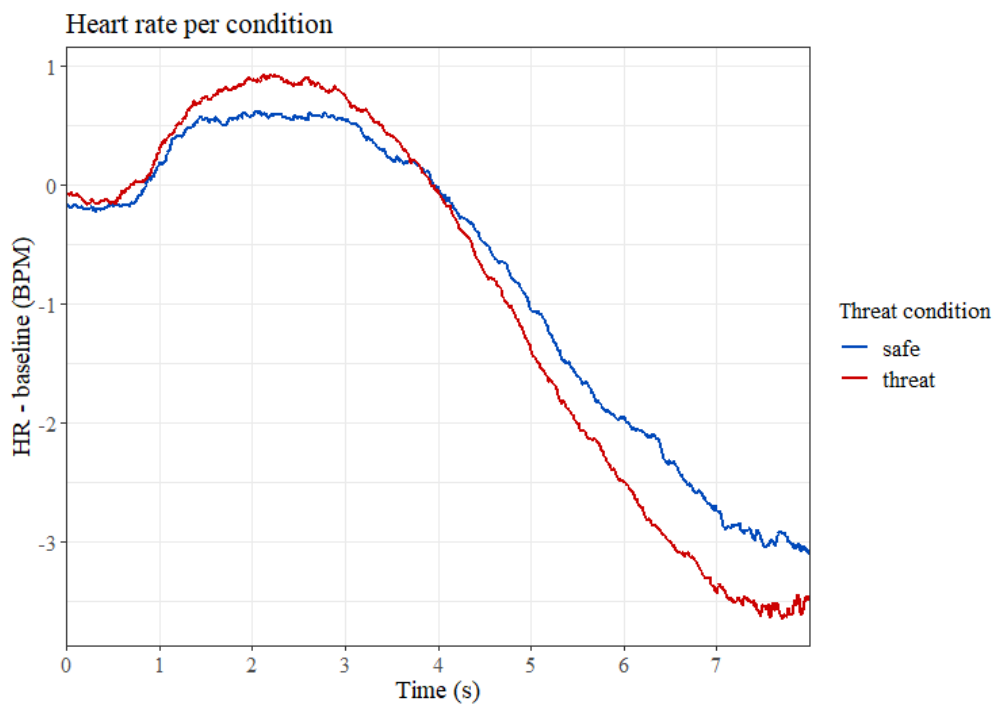

Figure 3: Conditional heart rate changes.

The figure represents the mean heart rate changes in beats per minute (BPM) after baseline correction. The red line reflects threat trials, and the blue line safe trials. A significant effect was found for time, and for the interaction between time and threat condition (3000-7000 ms). Threat versus safe conditions did not differ significantly in terms of heart rate deceleration.

3.3 MEG results

First of all, the MEG source-level results were compared between shoot and withhold trials. Here, we expected to see a clear motor response in shoot trials as a result of the button press. It is predicted that this motor response is accompanied by beta-band decreases and gamma-band increases in the sensorimotor cortex (Crone, 1998a,b). The aim of this first analysis was to check whether the MEG analyses, including source reconstruction, have been executed correctly. Secondly, the neural mechanisms underlying freeze were investigated, for which we hypothesised that freezing might be associated with increased theta-band rhythmic activity in the MCC. Finally, we explored the electrophysiological processes that are involved during the switch from freeze to action. As described earlier, we predicted that the switch from freezing to action is reflected in a shift from MCC to ACC activity, which might also release the SMC from inhibition.

3.3.1 Source-level analysis comparing shoot and withhold trials

The difference between correct shoot and withhold trials was examined by computing time-frequency representations, that were statistically compared by conducting a cluster-based permutation analysis over the first second after the draw. First, the analysis was performed using a frequency window ranging from 0 to 40 Hz. Positive effects represent the parts where the power of the signal is higher for threat compared to safe trials, while negative effects reflect the opposite. For all three regions, both significant positive and negative effects were found, indicating low-frequency power increases (e.g., alpha-band) and beta-band power decreases, respectively. In the MCC, a significant positive effect was observed depending on a cluster formed between 6 and 16 Hz, lasting from 50 to 300 ms ($p = 0.036$), whereas a significant negative effect was found based on a cluster ranging from 4 to 26 Hz between 350 and 1000 ms ($p = 0.0080$; see Figure 4A). For the ACC, a significant positive effect was found for a cluster between 4 and 16 Hz that persisted from 50 to 250 ms ($p = 0.042$), while a negative effect was perceived within the same frequency range but lasting from 500 to 1000 ms ($p = 0.0020$; see Figure 4B). Finally, analysis on the SMC showed that there is a significant positive effect based on a cluster formed between 0 and 8 Hz that lasted from 150 to 600 ms ($p = 0.030$), and a negative effect based on clustering from 4 to 34 Hz that covered the full time window ($p = 0.0020$; see Figure 4C).

A similar analysis was performed for frequencies between 40 and 150 Hz. Here, no significant conditional differences were found in the MCC and ACC (see Figure 4D,E). Conversely, both a positive and a negative effect were found in the SMC, the first one being observed between 60 and 150 Hz, persisting from 250 to 550 ms ($p = 0.0020$), and the latter between 40 and 60 Hz, lasting from 400 to 820 ms ($p = 0.022$; see Figure 4F).

The significant relative gamma-band increases and beta-band decreases that we observed correspond to previous findings on functional activity in the SMC (e.g., Crone, 1998a,b). Furthermore, the low-frequency power increases that we found are likely event-related fields, reflecting time-locked neural responses to the stimulus onset (Gross et al., 2013). We showed that the temporal on- and offset of the event-related fields differed per reconstructed region, as did the spectral range. Taken together, the motor-related activity observed in the SMC indicates that source reconstruction is executed correctly, whereas the variations in the event-related fields confirm that the three reconstructed areas are independent of each other.
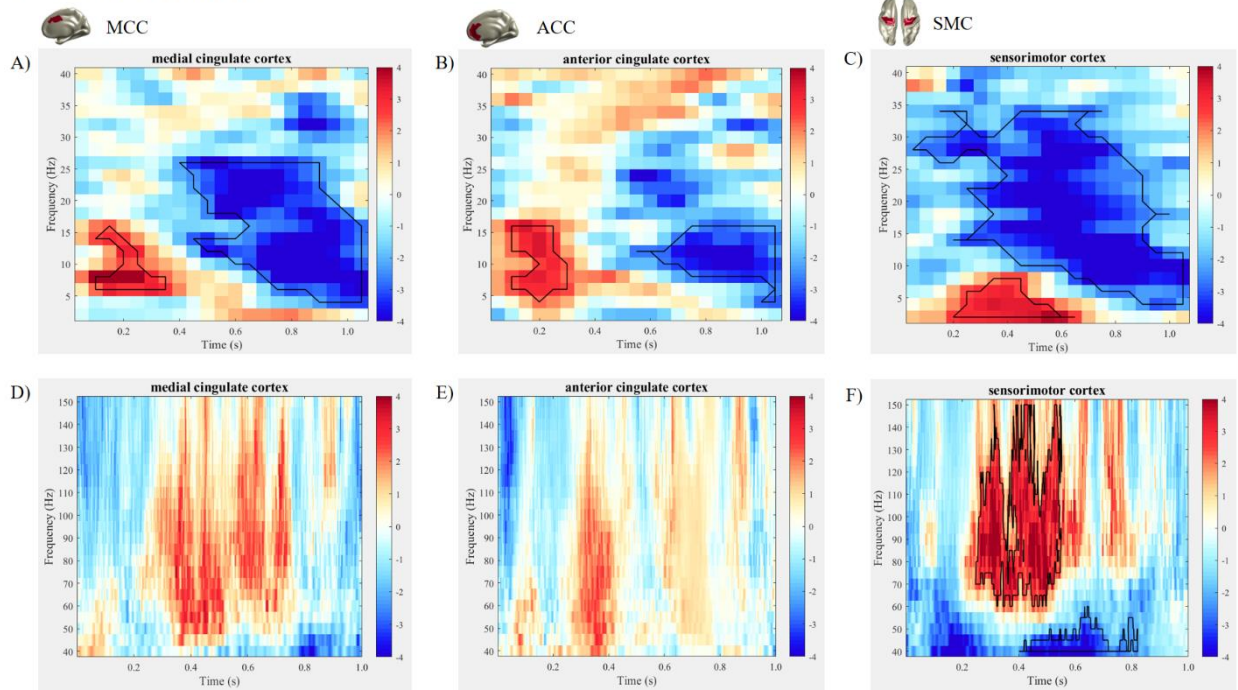
Figure 4: Time-frequency representation during the switch to action.

In this figure, t-values are plotted which reflect the relative power difference between correct shoot trials and correct withhold trials for MCC (A,D), ACC (B,E) and SMC (C,F) independently. The top row represents a frequency range between 0 and 40 Hz, the bottom row from 40 to 150 Hz. Time point zero is the moment the opponent performed an action. Red blobs indicate that threat trials evoked higher power, whereas the signal was stronger in safe trials for the blue areas. Significant effects are visualised with the black lines.

3.3.2 Anticipation window – power spectral density and connectivity

To reveal whether the frequency content of signals evoked by threat and safe trials were significantly different, the power spectral densities were compared over the whole anticipation period (6 - 9 sec per trial) by conducting a cluster-based permutation test. This yielded a significant effect in the MCC that was based on a cluster formed between 19 and 22 Hz ($p = 0.048$; see Figure 5A). Therefore, MCC activity seems to be modulated under threat of shock, which is in line with our hypotheses. However, we expected that the effect would manifest in theta-band rhythmic activity, whereas beta-band modulations were observed here. Furthermore, no significant conditional differences were observed in the ACC (see Figure 5B), which is in accordance with prior expectations. Finally, significant differences in the SMC were observed between 10 and 13 Hz ($p = 0.024$), and between 17 and 26 Hz ($p = 0.0060$; see Figure 5C). Here, it is shown that the power of the signal evoked by threat trials is decreased in the alpha- and beta- band, indicating a release from cortical inhibition that might be associated with action preparation.
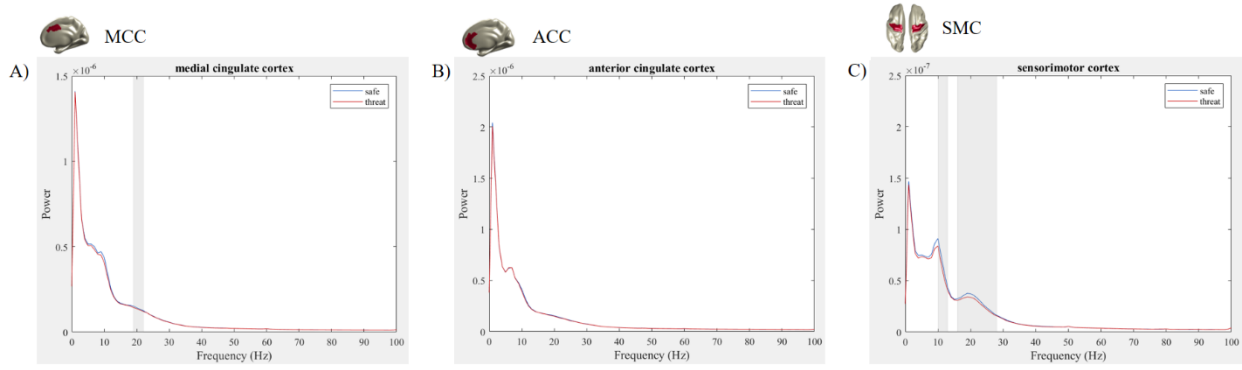
Safe versus threat (anticipation)

Figure 5: Power spectral density during the anticipation window.

The frequency content of the signal is represented during the anticipation of a threatening (red) or safe (blue) stimulus. A) Power spectrum for the MCC, the grey bar reflects a significant conditional difference that was observed between 19 and 22 Hz. B) Spectral density plot for signals generated by the ACC, revealing no significant conditional differences. C) Results for the SMC, showing a significant difference from 10 to 13 Hz, and from 17 to 23 Hz, as indicated by the grey bars.

To investigate whether there was communication between the three regions during freeze, a permutation test was conducted to compare the coherence and Granger causality spectra. Comparisons were made between threat and safe trials, revealing that coherence differed significantly between the MCC and SMC from 26 to 29 Hz (p = 0.010). This indicates that there is lower synchronized beta-band activity in the threat condition (see Figure 6). However, no significant effects were found in directional connectivity, which was computed according to the Granger causality test (see Figure 7). The results suggest that there are no threat-related differences in directional connectivity, which contradicts the prediction that the MCC communicates more strongly to the SMC under the threat of shock.

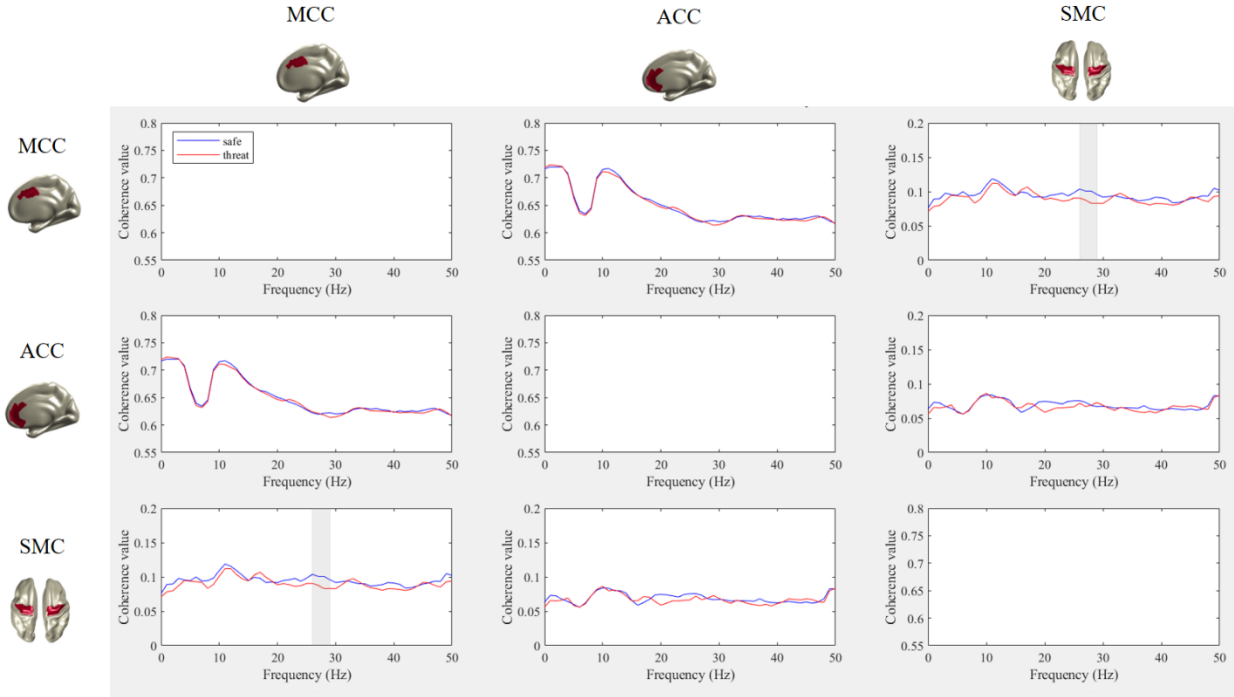## Coherence: threat versus safe (anticipation)

Figure 6: Coherence spectra during anticipation.

Coherence comparisons were made between the anticipation of a threatening (red lines) or safe (blue lines) cue. A significant effect was found between MCC and SMC from 26 to 29 Hz, which is indicated by the grey bars.

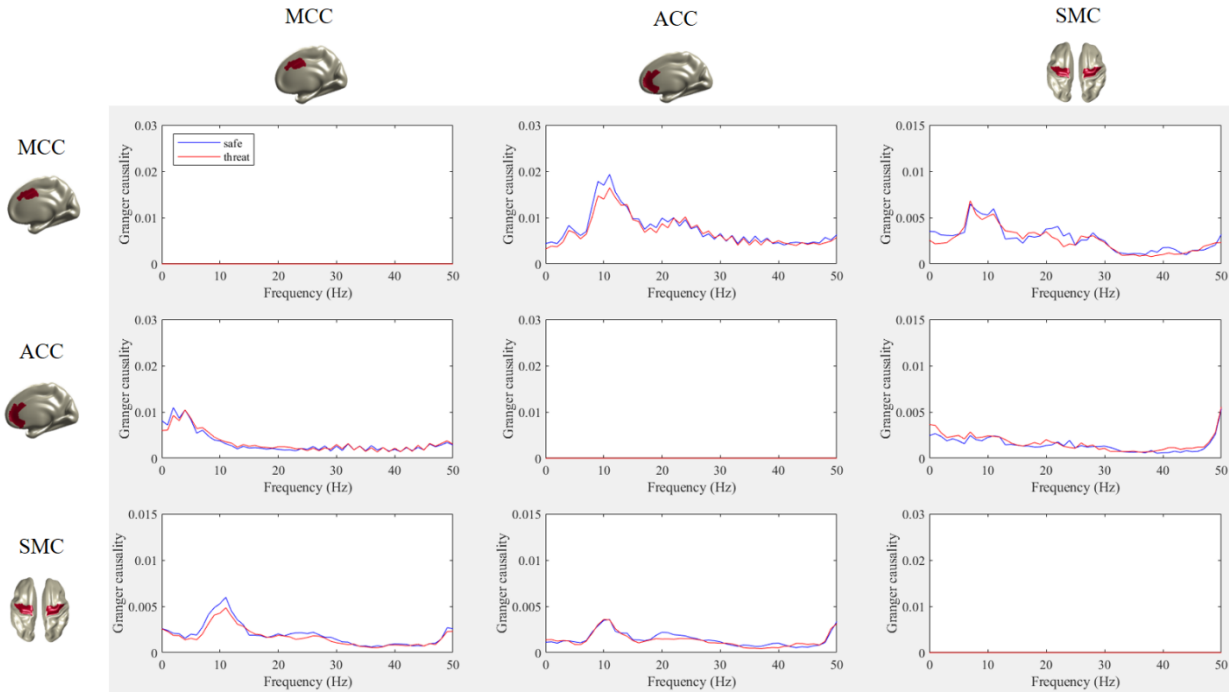## Granger causality: threat versus safe (anticipation)

Figure 7: Granger causality spectra during anticipation.

Directional connectivity was assessed by calculating Granger causality between each of the three regions. Red lines reflect anticipation of a threatening stimulus, whereas blue lines represent safe trials. No significant conditional differences could be observed.

3.3.3 Switch to action – time-frequency representation and connectivity

Regarding the switch from freeze to action, we examined if the time-frequency representations differed between correct shoot trials in the threat and safe condition. This was done in order to investigate whether the switch to action was modulated under threat of shock. Within a frequency range from 0 to 40 Hz, no clear conditional differences could be observed for any of the regions, which was confirmed by non-significant results on a cluster-based permutation test (see Figure 8A-C). Based on visual inspection, it can be seen that between 40 and 150 Hz, shoot trials elicit higher power compared to withhold trials in both cingulate cortices, where the effect appears to be strongest in the ACC. In the SMC, gamma-band power appears to be higher for shoot trials too, but the spectral range is lower than in the MCC and ACC. In line with the hypotheses, the largest conditional power differences could be observed in the ACC, suggesting that this region is involved in the switch from freeze to action. The results were compared statistically by means of a cluster-based permutation test, but this yielded no significant differences in any of the regions (see Figure 8D-F).
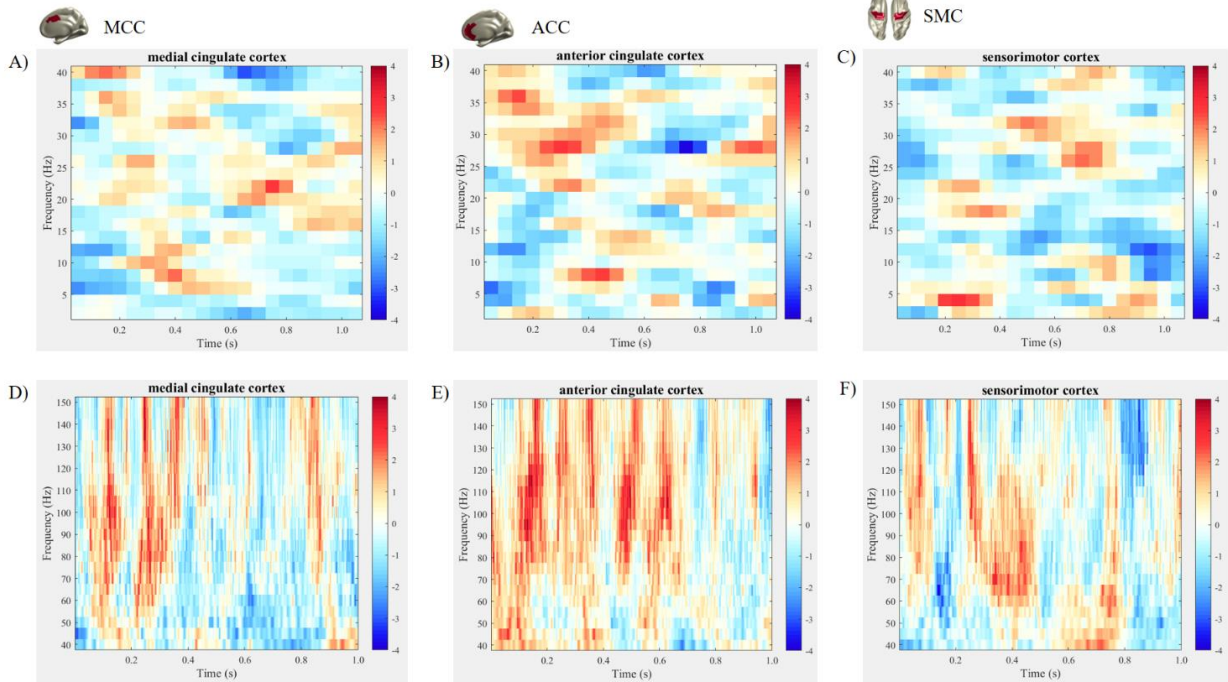

Figure 8: Time-frequency representation during the switch to action.

Relative power differences (t-values) are visualised comparing the switch to action in a threatening and safe situation. The top row contains frequencies between 0 and 40 Hz, the bottom row between 40 and 150 Hz. The draw is initiated at time point zero. The red parts reflect where power is higher for signals evoked by threat trials. None of the regions - MCC (A,D), ACC (B,E), and SMC (C,F) - showed a significant conditional difference.

Subsequently, connectivity patterns were compared during the draw, for which comparisons were made between correct shoot trials in the threat and safe condition. Here, no significant differences were observed regarding the coherence between conditions (see Figure 9). However, a significant effect was perceived in directional connectivity from MCC to SMC between 28 and 30 Hz ($p = 0.030$), indicating that communication through beta-band rhythms is decreased in safe compared to threat trials (see Figure 10). This finding might suggest that SMC is released from MCC inhibition during the switch from freeze to action, which would correspond to our prior expectations.

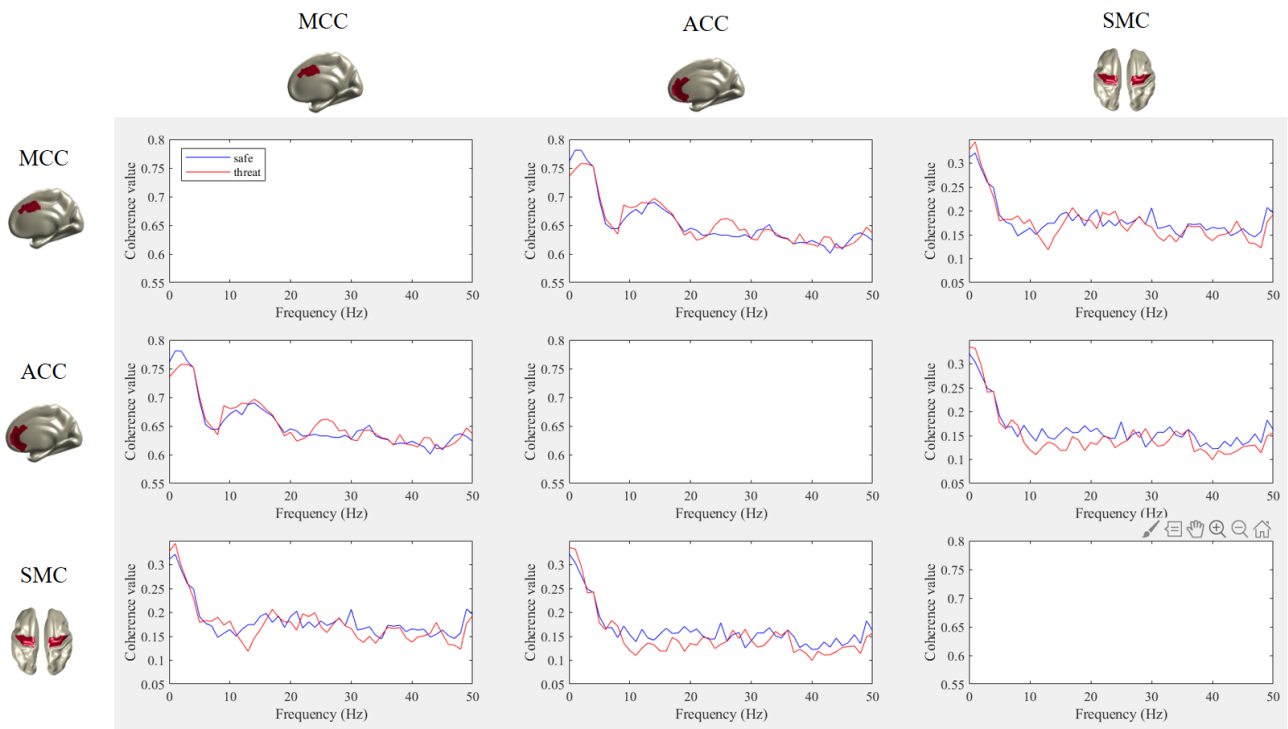**Coherence: threat shoot versus safe shoot (switch to action)**

Figure 9: Coherence spectra during the switch to action.

Coherence spectra were compared between correct shoot trials in the threat (red lines) and safe (blue lines) condition. No significant difference could be found between any of the regions.

Granger causality: threat shoot versus safe shoot (switch to action)
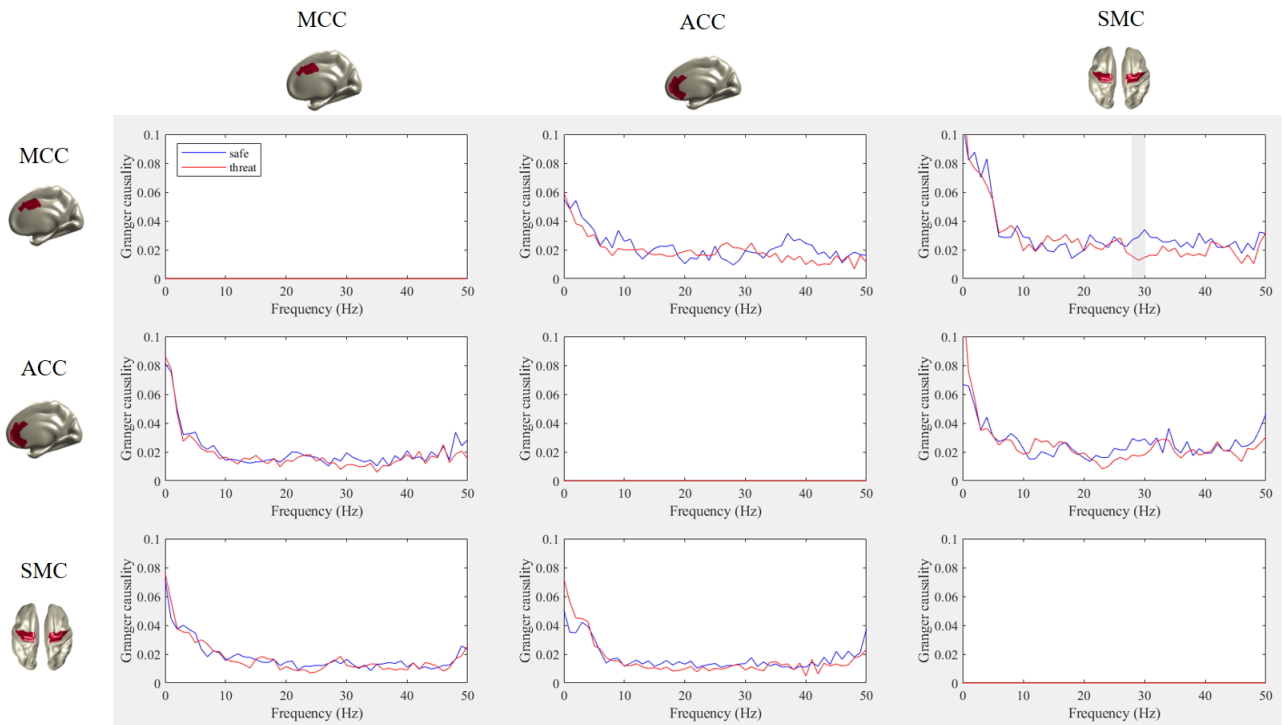

Figure 10: Granger causality spectra during the switch to action.

Granger causality was calculated for each possible combination of regions. Again, threat (red) and safe (blue) shoot trials were compared, and a significant effect could be observed from MCC to ACC, ranging from 28 to 30 Hz.

4. Discussion

This study examined the neural mechanisms underlying freeze and the subsequent switch to action. The findings demonstrated that the anticipation of a threatening stimulus was associated with reduced beta-band power in the MCC, as well as decreased alpha- and beta-band power in the SMC. Furthermore, during the switch to action, we observed (non-significant) increases in gamma-band activity in the ACC for threat compared to safe trials. Finally, we showed that directional connectivity from MCC to SMC was decreased during the switch from freeze to action. Taken together, the findings demonstrated that freezing is associated with enhanced action preparation as reflected by releases from cortical inhibition in the alpha and beta-band rhythmic activity. Additionally, our results suggest that the ACC is involved during the switch from freeze to action, which is potentially implemented through a release from MCC to SMC inhibition.

Behavioural and physiological effects of threat manipulation

We used a shooting task to imitate real-life threat by having participants make rapid decisions under the threat of shock. The behavioural results were similar to the results of a previous study that used the same paradigm. Namely, when comparing threat to safe trials, participants were more accurate on shoot trials while they performed worse on withhold trials (Hashemi et al., 2019a,b). This suggests that threat has been manipulated successfully during the experimental task. Furthermore, heart rate decelerations were calculated to see whether freezing was indeed elicited during threat trials. Although a significant interaction effect between threat condition and time was found, none of the time points indicated a significant difference between threat and safe trials after conducting post-hoc paired samples t-tests. This does not fully replicate previous findings that showed significantly stronger heart rate decreases for threat compared to safe trials towards the end of the anticipation interval (Gladwin et al., 2016; Hashemi et al., 2019a,b). A potential explanation for this finding can be that the current study is statistically underpowered.

Alternatively, our result could be explained by individual variations in freezing response. To illustrate, when looking at the heart rate results at the individual level, threat-related bradycardia could only be observed in half of the subjects. These interpersonal differences in defensive stress reactions could be linked to individual differences in anxiety or aggression, or variation in having experienced prior aversive life events (Niermann, Figner & Roelofs, 2017; Hagenaars, Stins & Roelofs, 2012). For subsequent analyses, these interindividual variations can be controlled for by correlating the results with outcomes of questionnaires approximating these factors, for example the State-Trait Anxiety Inventory (STAI; Spielberger, 1983).

To see whether our heart rate results affected the electrophysiological outcomes on freeze, supplementary analyses were performed including only the individuals who showed bradycardia (see Supplementary Materials S2).

Neural mechanisms underlying threat-anticipation

To address the neural mechanisms underlying freeze, power spectral density analyses were performed to reveal the frequency content of signals evoked by the MCC, ACC and SMC. Here, the most pronounced result are the threat-related reductions in alpha and beta-band rhythmic activity in the SMC. We suggest that this reflects action preparation, which is supported by previous findings showing that decreased alpha- and beta-band power was associated with disinhibition of the sensorimotor cortex (Stolk et al., 2019). This is in line with previous results indicating that freezing can be seen as an active preparatory state (Gladwin et al., 2016; Hashemi et al., 2019a). Moreover, this study provides the first electrophysiological evidence that freezing involves threat-induced inhibition of the sensorimotor cortex in humans. This finding confirms – at the neural level – the idea that freezing is related to action preparation (Roelofs, 2017).

Furthermore, a significant threat-related modulation was observed in the MCC during anticipation, demonstrating that beta-band power was lower for the threat compared to the safe condition. Consistent with previous work, threat manipulation has been shown to alter MCC involvement during threat anticipation (Hashemi et al., 2019a). The observed decrease in beta-band power can be interpreted as a release from cortical inhibition, which may reflect continuous updating of action plans (shooting or withholding) during threat-anticipation (Hosaka, Nakajima, Aihara, Yamaguchi & Mushiake, 2015).

However, previous findings suggested that threat-related alterations could manifest as a gain in theta-band rhythmic activity (Grunfeld & Likhtik, 2018), rather than in the observed beta-band power. Additionally, it has been hypothesised that the MCC could generate fear-evoked theta-band rhythms to communicate to the SMC to enable action preparation during freeze (Stujenske et al., 2014; Grunfeld & Likhtik, 2018). Yet, the current study did not show any threat-related modulations within the theta frequency band. This null-finding could be explained by the fact that the hypotheses related to theta-band activity were mainly based on previous rodent studies. Therefore, the lack of theta-related findings can be the result of fundamental differences between the rodent and human cingulate cortex. For example, the subregions of the rodent cingulate cortex could be partitioned inconsistently with the human cingulate cortex, for which it may be possible that our regions of interest were nonhomologous to the rodent's areas that were found previously (van Heukelum et al., 2020).

Finally, significant connectivity differences have been observed for the coherence spectra between MCC and SMC in the beta-band (26-29 Hz). Coherence between these regions in general could be explained by the fact that there is strong anatomical connectivity between the MCC and SMC (Van Heukelum et al., 2020). Nevertheless, this should not affect the conditional differences, for which it is presumable that the observed effect is due to other factors. For instance, it could be that the found coherence difference is spurious, due to condition-related variations in the amplitude of the sources. Indeed, the power spectral density shows that beta-band rhythmic activity is significantly different between the two threat conditions. Therefore, it is likely that the coherence difference in the beta-band rhythms is the result of beta-band power decreases in the threat compared to the safe condition.

Electrophysiology underlying the switch to action

Regarding the switch to action, we first made spectro-temporal comparisons between trials where an action was executed and trials in which participants withheld their response. This yielded significantly higher gamma-band rhythmic activity, as well as reduced beta-band rhythmic activity at the moment an action was being performed. This pattern of activity is associated with cortical activation and is consistent with previous findings that reflect motor activity (Crone, 1998a,b). Furthermore, the positive clusters that were perceived between 0 and 40 Hz represented event-related fields that reflect neural responses that are time-locked to the stimulus-presentation (Gross et al., 2013). The fact that the event-related fields had different temporal and spectral on- and offsets confirmed that three independent regions were reconstructed successfully.

Secondly, when comparing shoot trials between the threat and safe condition, it was expected that the ACC elicited stronger activity in the threat condition at the expense of MCC activation (Hashemi et al., 2019a; Grunfeld & Likhtik, 2018). This could be explained by the idea that the ACC is responsible for the switch from freezing to action (Etkin, Egner & Kalisch, 2011). Here, we indeed observed (non-significant) increases in gamma-band activity in the ACC, prior to the response and response-related effects in the SMC, which may reflect increased neuronal synchronization during fear-related behaviour (Rozeske & Herry, 2018). Based on this, we speculate that there is increased involvement of the ACC during the switch to action, which would be in line with our hypotheses. Furthermore, significant decreased directional connectivity from the MCC to the SMC was found in the beta-band during threat trials, which could be interpreted as a release from MCC to SMC cortical inhibition. Taken together, although the increases in ACC activity were not significant, the observations did resemble what we would expect based on previous work (e.g., Grunfeld & Likthik, 2018; Hashemi et al., 2019). Namely, the ACC seems to take over MCC activity during the switch to action, which is accompanied by disinhibition of the SMC to allow action execution.

Finally, during the draw, it was predicted that there is directional connectivity from the ACC to SMC to initiate an action. The fact that no directional activity was found from ACC to SMC suggests that the neural communication is implemented in a different way. For example, the ACC may communicate to the amygdala to shut down their inputs, after which the initiation of an action can be signalled by releasing MCC to SMC inhibition (Grunfeld & Likhtik, 2018).

Interpretational issues

A first limitation of the current study is the reduced statistical power due to a small sample size. To illustrate, the power calculation for this research showed that 46 participants are needed to reach a medium effect size with 80% power (d = 0.38, based on Hashemi et al., 2019b). However, only 26 participants were tested so far, of which 24 participants were included in the analyses. As a result, the sample size is too small to find powerful and reliable results. Therefore, it is important to repeat the analyses on the final sample size in order to draw correct conclusions.

Furthermore, the analyses that we performed were based on previous findings on defensive freezing. To quantify if freezing was elicited, threat-related bradycardia was calculated. Although some participants showed strong heart rate decelerations, bradycardia in the threat condition did not appear to be significantly stronger on the group level at the end of the anticipation window. As a result, the current research addresses the switch from threat-anticipation to action, rather than the switch from freezing to action. To reveal if the results generalize to freezing, further research should focus on trial-level correlations between heart rate deceleration and the electrophysiological measures.

Thirdly, to investigate the involvement of the MCC, ACC and SMC during freeze and the switch to action, we reconstructed these sources of interest by creating virtual channels. Here, each reconstructed region included both the left and right cortices of the relevant source. However, since participants only responded with their right hand during the task, action-related activity is expected to be most prevalent in the left motor cortex. Hence, our reconstructed source comprising the bilateral sensorimotor cortex might be too large, reducing the power of the activity related to action preparation and execution. Furthermore, MCC and ACC activity might be stronger in the left hemisphere, as is their potential communication to the SMC. Therefore, future research should consider the respective left and right cortices as separate sources, in order to more specifically reveal the neural mechanisms underlying freezing as an active state.

Finally, the current study addressed the neural mechanisms underlying the switch from freeze to action by focusing on the MCC, ACC and SMC. However, the neural network involved in freezing and the consequent switch to action also includes subcortical regions such as the amygdala, periaqueductal gray (PAG), hypothalamus and other midbrain regions (Hashemi et al., 2019a; Roelofs, 2017; Hagenaars et al., 2014; Misslin, 2003; Fendt & Fanselow, 1999). It is indicated that the subnuclei of these regions encode either passive or active defensive behaviours, through which this subcortical network is likely to be involved in the flexible switching from freeze to action as well (Hagenaars et al., 2014). For this reason, future investigations should also involve subcortical regions to provide a comprehensive overview of the neural mechanisms underlying the switch from freeze to action.

Conclusion

Taken together, the current study explored the electrophysiological mechanisms underlying freezing and the switch from freezing to action. The findings showed that freezing is associated with enhanced action preparation, which is manifested through decreased alpha- and beta-band rhythmic activity. Furthermore, our results suggest that the ACC is involved during the switch to action, and that this switch is associated with a release from MCC to SMC inhibition, facilitating quick action responses. Although re-analysis with increased sample size is needed for a more reliable overview of the involved neural mechanisms, the current study advances our knowledge of freezing and its relation to action preparation and execution. This understanding can contribute to the improvement of training programs for humans in high-risk professions, and ultimately to enhance their performance under threat.

5. References

Bastos, A. M. & Schoffelen, J. M. (2016). A Tutorial Review of Functional Connectivity Analysis Methods and Their Interpretational Pitfalls. *Frontiers in Systems Neuroscience*, *9.* https://doi.org/10.3389/fnsys.2015.00175

Crone, N. (1998a). Functional mapping of human sensorimotor cortex with electrocorticographic spectral analysis. I. Alpha and beta event- related desynchronization. *Brain, 121*(12), 2271–2299. https://doi.org/10.1093/brain/121.12.2271

Crone, N. (1998b). Functional mapping of human sensorimotor cortex with electrocorticographic spectral analysis. II. Event-related synchronization in the gamma-band. *Brain, 121*(12), 2301–2315. https://doi.org/10.1093/brain/121.12.2301

Etkin, A., Egner, T. & Kalisch, R. (2011). Emotional processing in anterior cingulate and medial prefrontal cortex. *Trends in Cognitive Sciences, 15*(2), 85–93. https://doi.org/10.1016/j.tics.2010.11.004

Fendt, M. & Fanselow, M. (1999). The neuroanatomical and neurochemical basis of conditioned fear. *Neuroscience & Biobehavioral Reviews, 23*(5), 743–760. https://doi.org/10.1016/s0149-7634(99)00016-0

Fries, P. (2005). A mechanism for cognitive dynamics: neuronal communication through neuronal coherence. *Trends in Cognitive Sciences, 9*(10), 474–480. https://doi.org/10.1016/j.tics.2005.08.011

Gladwin, T. E., Hashemi, M. M., van Ast, V. & Roelofs, K. (2016). Ready and waiting: Freezing as active action preparation under threat. *Neuroscience Letters, 619*, 182–188. doi.org/10.1016/j.neulet.2016.03.027

Glasser, M. F., Coalson, T. S., Robinson, E. C., Hacker, C. D., Harwell, J., Yacoub, E., Ugurbil, K., Andersson, J., Beckmann, C. F., Jenkinson, M., Smith, S. M. & Van Essen, D. C. (2016). A multi-modal parcellation of human cerebral cortex. *Nature*, *536*(7615), 171–178. https://doi.org/10.1038/nature18933

Gross, J., Baillet, S., Barnes, G. R., Henson, R. N., Hillebrand, A., Jensen, O., Jerbi, K., Litvak, V., Maess, B., Oostenveld, R., Parkkonen, L., Taylor, J. R., van Wassenhove, V., Wibral, M. & Schoffelen, J. M. (2013). Good practice for conducting and reporting MEG research. *NeuroImage, 65*, 349–363. https://doi.org/10.1016/j.neuroimage.2012.10.001

Grunfeld, I. S. & Likhtik, E. (2018). Mixed selectivity encoding and action selection in the prefrontal cortex during threat assessment. *Current Opinion in Neurobiology, 49*, 108–115. doi.org/10.1016/j.conb.2018.01.008

Hagenaars, M. A., Oitzl, M. & Roelofs, K. (2014). Updating freeze: Aligning animal and human research. *Neuroscience & Biobehavioral Reviews*, *47*, 165–176. doi.org/10.1016/j.neubiorev.2014.07.021

Hagenaars, M. A., Stins, J. F. & Roelofs, K. (2012). Aversive life events enhance human freezing responses. Journal of Experimental Psychology: *General, 141*(1), 98–105. https://doi.org/10.1037/a0024211

Hashemi, M. M., Gladwin, T. E., de Valk, N. M., Zhang, W., Kaldewaij, R., van Ast, V., … Roelofs, K. (2019a). Neural Dynamics of Shooting Decisions and the Switch from Freeze to Fight. *Scientific Reports, 9*(1). doi.org/10.1038/s41598-019-40917-8

Hashemi, M. M., Zhang, W., Kaldewaij, R., Koch, S. B. J., Jonker, R., Figner, B., Klumpers, F. & Roelofs, K. (2019b). Human defensive freezing is associated with acute threat coping, long term hair cortisol levels and trait anxiety. *BioRxiv*, 12–13. https://doi.org/10.1101/554840

Hosaka, R., Nakajima, T., Aihara, K., Yamaguchi, Y. & Mushiake, H. (2015). The Suppression of Beta Oscillations in the Primate Supplementary Motor Complex Reflects a Volatile State During the Updating of Action Sequences. *Cerebral Cortex, 26*(8), 3442–3452. https://doi.org/10.1093/cercor/bhv163

Jensen, O. & Mazaheri, A. (2010). Shaping Functional Architecture by Oscillatory Alpha Activity: Gating by Inhibition. *Frontiers in Human Neuroscience*, *4*. https://doi.org/10.3389/fnhum.2010.00186

Karalis, N., Dejean, C., Chaudun, F., Khoder, S., Rozeske, R. R., Wurtz, H., Bagur, S., Benchenane, K., Sirota, A., Courtin, J. & Herry, C. (2016). 4-Hz oscillations synchronize prefrontal–amygdala circuits during fear behavior. *Nature Neuroscience, 19*(4), 605–612. doi.org/10.1038/nn.4251

Klumpers, F., Raemaekers, M. A., Ruigrok, A. N., Hermans, E. J., Kenemans, J. L. & Baas, J. M. (2010). Prefrontal Mechanisms of Fear Reduction After Threat Offset. *Biological Psychiatry, 68*(11), 1031–1038. https://doi.org/10.1016/j.biopsych.2010.09.006

Lojowska, M., Gladwin, T. E., Hermans, E. J. & Roelofs, K. (2015). Freezing promotes perception of coarse visual features. *Journal of Experimental Psychology: General, 144*(6), 1080–1088. doi.org/10.1037/xge0000117

Lojowska, M., Ling, S., Roelofs, K. & Hermans, E. J. (2018). Visuocortical changes during a freezing-like state in humans. *NeuroImage, 179*, 313–325. https://doi.org/10.1016/j.neuroimage.2018.06.013

Lojowska, M., Mulckhuyse, M., Hermans, E. J. & Roelofs, K. (2019). Unconscious processing of coarse visual information during anticipatory threat. *Consciousness and Cognition*, *70*, 50–56. https://doi.org/10.1016/j.concog.2019.01.018

Maris, E. (2011). Statistical testing in electrophysiological studies. *Psychophysiology, 49*(4), 549–565. https://doi.org/10.1111/j.1469-8986.2011.01320.x

Maris, E. & Oostenveld, R. (2007). Nonparametric statistical testing of EEG- and MEG-data. *Journal of Neuroscience Methods, 164*(1), 177–190. https://doi.org/10.1016/j.jneumeth.2007.03.024

Misslin, R. (2003). The defense system of fear: behavior and neurocircuitry. Neurophysiologie *Clinique/Clinical Neurophysiology, 33*(2), 55–66. https://doi.org/10.1016/s0987-7053(03)00009-1

Niermann, H. C., Figner, B. & Roelofs, K. (2017). Individual differences in defensive stress-responses: the potential relevance for psychopathology. *Current Opinion in Behavioral Sciences, 14*, 94–101. https://doi.org/10.1016/j.cobeha.2017.01.002

Oostenveld, R., Fries, P., Maris, E. & Schoffelen, J.-M. (2011). FieldTrip: Open Source Software for Advanced Analysis of MEG, EEG, and Invasive Electrophysiological Data. *Computational Intelligence and Neuroscience, 2011*, 1–9. doi.org/10.1155/2011/156869

Roelofs, K. (2017). Freeze for action: neurobiological mechanisms in animal and human freezing. *Philosophical Transactions of the Royal Society B: Biological Sciences, 372*(1718). doi.org/10.1098/rstb.2016.0206

Roelofs, K., Hagenaars, M. A. & Stins, J. (2010). Facing Freeze: Social Threat Induces Bodily Freezing in Humans. *Psychological Science*, *21*(11), 1575–1581. doi.org/10.1177/0956797610384746

Rozeske, R. R. & Herry, C. (2018). Neuronal coding mechanisms mediating fear behavior. *Current Opinion in Neurobiology, 52*, 60–64. https://doi.org/10.1016/j.conb.2018.04.017

Spielberger, C. D. (1983). State-Trait Anxiety Inventory for Adults. *PsycTESTS Dataset*. Published. https://doi.org/10.1037/t06496-000

Stolk, A., Brinkman, L., Vansteensel, M. J., Aarnoutse, E., Leijten, F. S. S., Dijkerman, C. H., … Toni, I. (2019). Electrocorticographic dissociation of alpha and beta rhythmic activity in the human sensorimotor system. *ELife*, *8*. https://doi.org/10.7554/elife.48065

Stolk, A., Todorovic, A., Schoffelen, J. M. & Oostenveld, R. (2013). Online and offline tools for head movement compensation in MEG. *NeuroImage, 68*, 39–48. https://doi.org/10.1016/j.neuroimage.2012.11.047

Stujenske, J. M., Likhtik, E., Topiwala, M. A. & Gordon, J. A. (2014). Fear and Safety Engage Competing Patterns of Theta-Gamma Coupling in the Basolateral Amygdala. *Neuron, 83*(4), 919–933. doi.org/10.1016/j.neuron.2014.07.026

van Heukelum, S., Mars, R. B., Guthrie, M., Buitelaar, J. K., Beckmann, C. F., Tiesinga, P. H. E., Vogt, B. A., Glennon, J. C. & Havenith, M. N. (2020). Where is Cingulate Cortex? A Cross-Species View. *Trends in Neurosciences, 43*(5), 285–299. doi.org/10.1016/j.tins.2020.03.007

van Veen, B., Van Drongelen, W., Yuchtman, M. & Suzuki, A. (1997). Localization of brain electrical activity via linearly constrained minimum variance spatial filtering. *IEEE Transactions on Biomedical Engineering, 44*(9), 867–880. https://doi.org/10.1109/10.623056

6. Supplementary

S1. Supplementary materials

	MCC	ACC	SMC
	MCC	ACC	SMC
Parcellation label	L_24_B05_03 / R_24_B05_03 L_32_B05_02 / R_32_B05_02	L_24_B05_04 / R_24_B05_04 L_24_B05_05 / R_24_B05_05 L_32_B05_01 / R_32_B05_01 L_32_B05_03 / R_32_B05_03	L_4_B05_01 / R_4_B05_01 L_4_B05_03 / R_4_B05_03 L_4_B05_05 / R_4_B05_05 L_4_B05_06 / R_4_B05_06 L_4_B05_07 / R_4_B05_07 L_4_B05_08 / R_4_B05_08 L_4_B05_12 / R_4_B05_12
Brodmann	Area a24',a24c' Area a32	Area 24c, p24, s24 Area p32, s32	Area 4

Figure S1: virtual channels – MCC, ACC, and SMC.

The medial cingulate cortex (MCC), anterior cingulate cortex (ACC) and sensorimotor cortex (SMC) were reconstructed on the source level. The regions of interest were spatially defined using a multimodal parcellation atlas (Glasser et al., 2016). The figure shows which subregions were included per virtual channel, as well as the corresponding Brodmann areas.

S2. Supplementary results

Participants performed a shooting task which measured action preparation under the threat of shock (Gladwin et al., 2016; Hashemi et al., 2019a,b). Here, heart rate deceleration (bradycardia) was calculated as a measure of freeze. The heart rate changes were visually inspected at the individual level, revealing threat-related bradycardia for eleven subjects. Supplementary analyses were performed to explore the electrophysiological mechanisms underlying the switch from freeze to action, by only including participants who showed threat-related bradycardia.

S2.1 Anticipation window – power spectral density and connectivity

First, the frequency content of the signals was computed by performing power spectral density analyses over the anticipation period. The results are visualised in Figure S2. The most pronouncing conditional difference is observed in the sensorimotor cortex, showing that the power is lower for threat trials in alpha- and beta-band rhythmic activity. Furthermore, there appears to be no conditional difference in power density for signals elicited by the MCC or ACC. These findings are consistent with the results observed from the analyses that included all participants (see Figure 5).
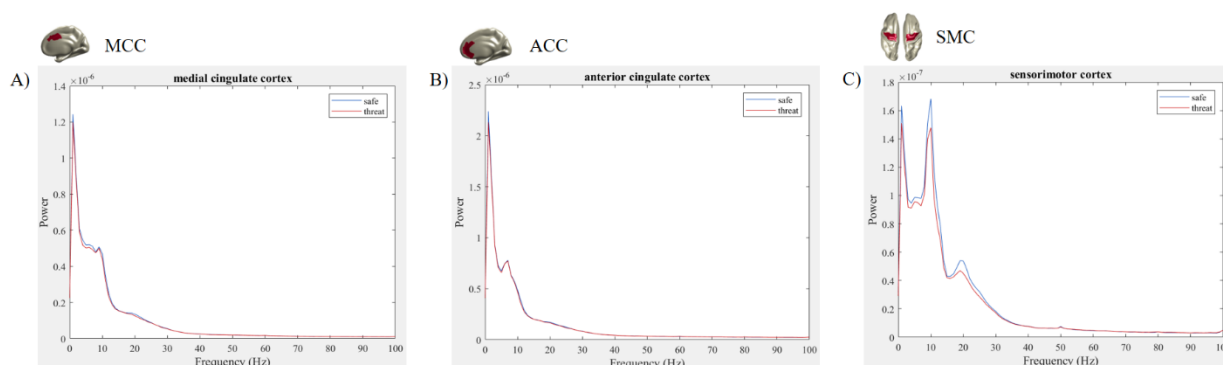

Freeze only: safe versus threat (anticipation)

Figure S2: Power spectral density during anticipation window – freeze only.

Power spectral density of the signal is represented during the anticipation of a threatening (red) or safe (blue) stimulus. The results were visualised for the MCC (A), ACC (B) and SMC (C) separately.

Additionally, connectivity measures were calculated for participants who froze during threat-anticipation. First, coherence spectra were computed, and thereafter we assessed directional connectivity using Granger causality. For both measures, there seems to be a slightly larger difference in connectivity between threat and safe trials (see Figure S3,S4). Based on visual inspection, it appears that these conditional differences are not manifested in a specific frequency range. Therefore, the results are comparable to the previous findings including the whole sample size (see Figure 6,7).
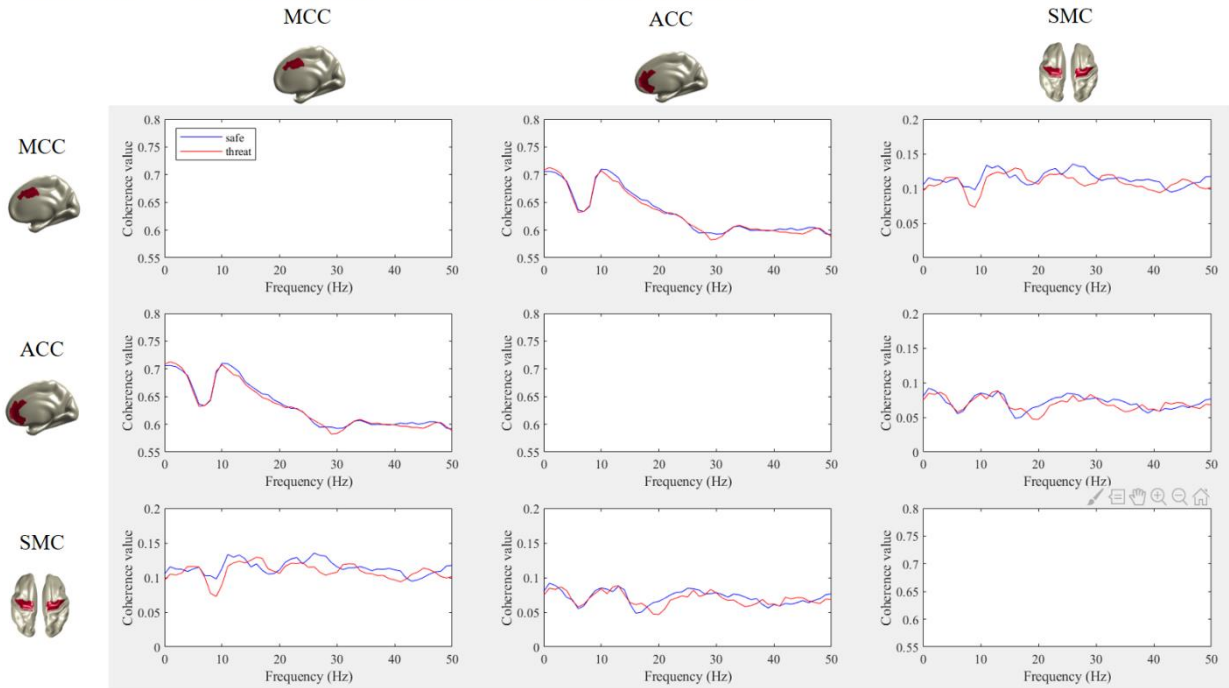
Figure S3: Coherence spectra during anticipation – freeze only.

Coherence spectra were compared between the anticipation of a threatening (red) or safe (blue) cue.
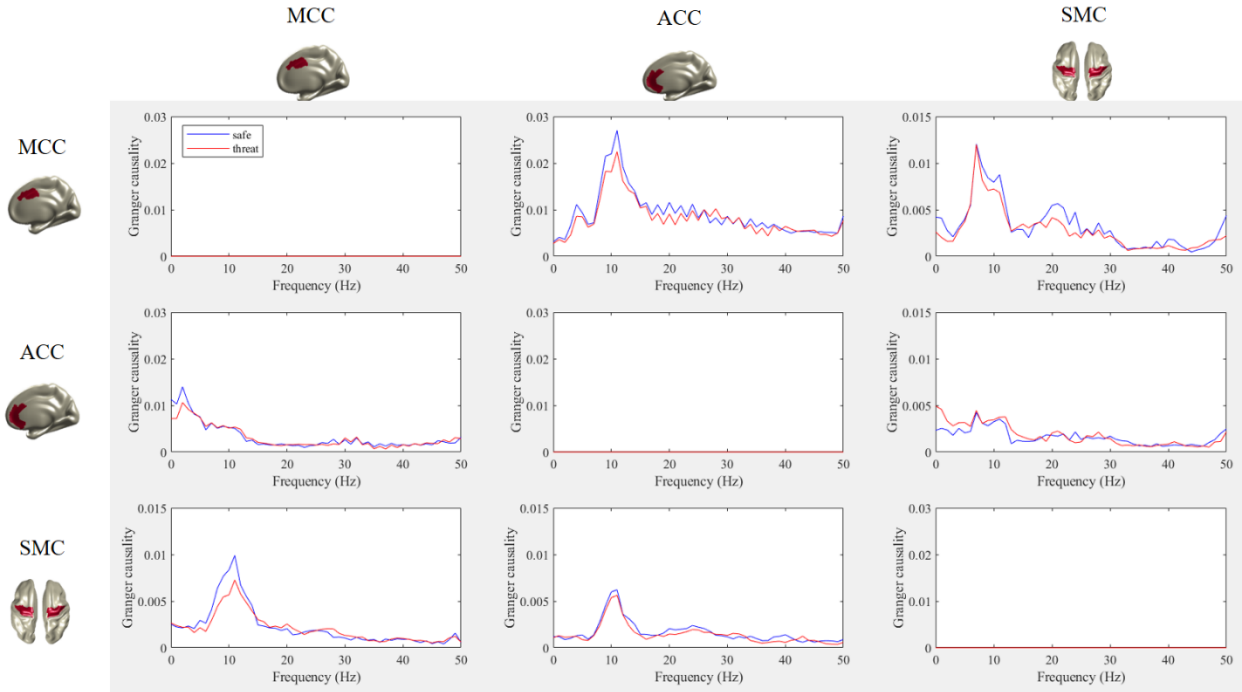

Figure S4: Granger causality spectra during anticipation - freeze only.

Directional activity is visualised,comparing the anticipation of a threatening (red) and safe (blue) cue.

S2.1 Switch to action – time-frequency representation and connectivity

Here, we examined if the time-frequency representations differed between correct shoot trials in the threat compared to the safe condition. The time-frequency representations were first visualised including the data of all participants (see Figure S5), and repeated including only the participants who froze (see Figure S6). We observed that threat-related gamma-band power is higher for the latter analysis, suggesting that freezing leads to enhanced involvement of the MCC, ACC and SMC during the switch to action. Furthermore, in both groups, threat-related power seems to be strongest in the ACC, which is in line with previous work suggesting that the ACC is responsible for the switch to action (e.g., Hashemi et al., 2019).
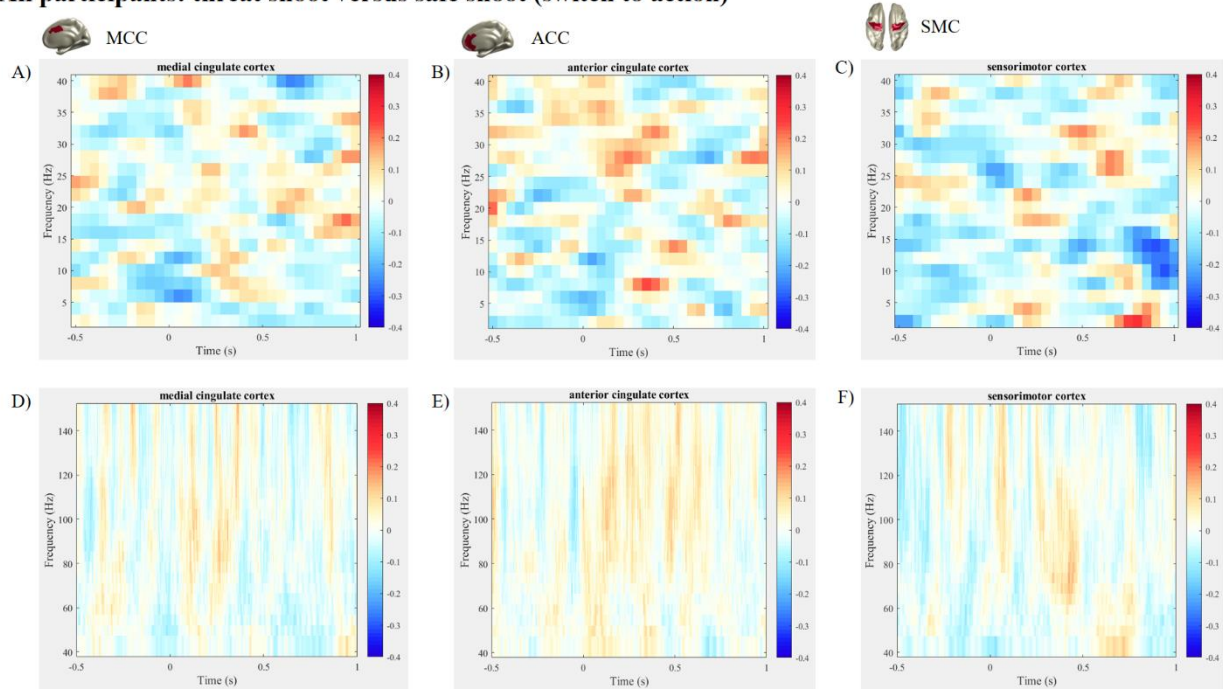

Figure S5: Time-frequency representation during the switch to action – all participants.

Relative power differences are plotted comparing the switch to action in a threatening and safe situation. The top row contains frequencies between 0 and 40 Hz, the bottom from between 40 and 150 Hz. .

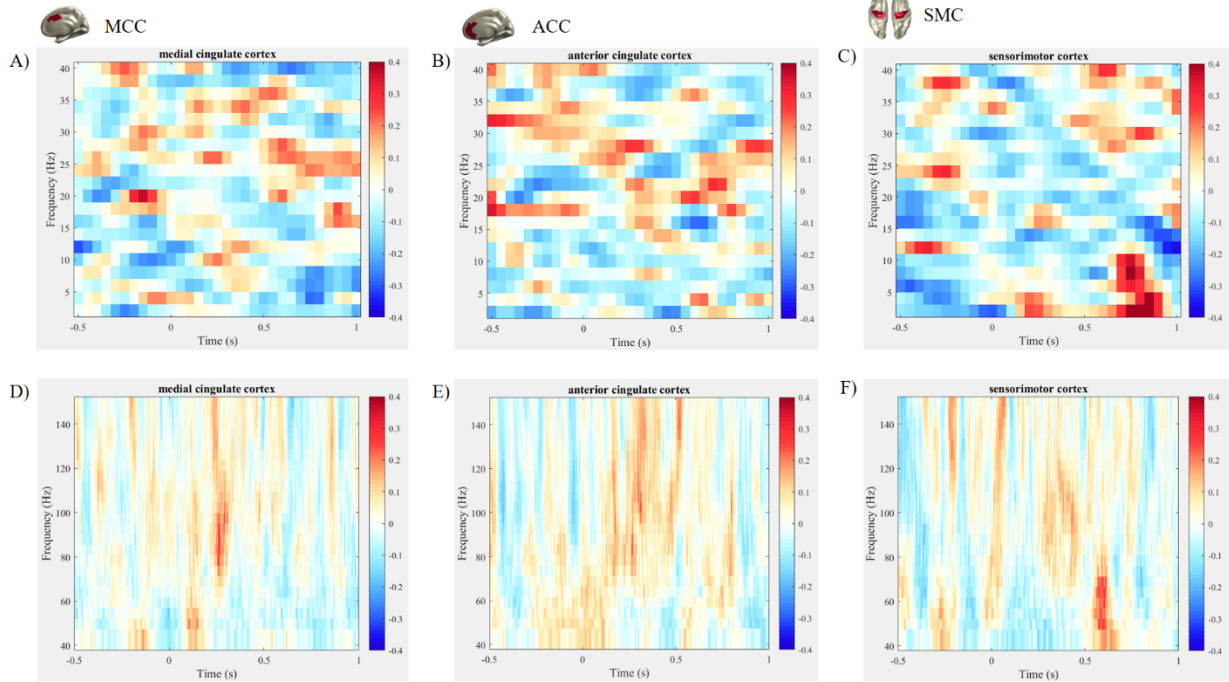**Freeze only: threat shoot versus safe shoot (switch to action)**

Figure S6: Time-frequency representation during the switch to action - freeze only.

Relative power differences are plotted only for participants who showed threat-related bradycardia. Threat and safe trials are compared during the switch to action. The top row contains frequencies between 0 and 40 Hz, the bottom from between 40 and 150 Hz.

Finally, connectivity analyses were performed during the draw by calculating coherence and Granger causality spectra. For both analyses, it appears that the conditional differences in connectivity are larger for participants who showed threat-related bradycardia (see Figure S7,S8). Therefore, it is suggested that freezing modulates connectivity between MCC, ACC and SMC. Furthermore, the pattern of connectivity looks similar to what is obtained from analyses including the whole sample size (see Figure 9,10).

Coherence – freeze only: threat shoot versus safe shoot (switch to action)
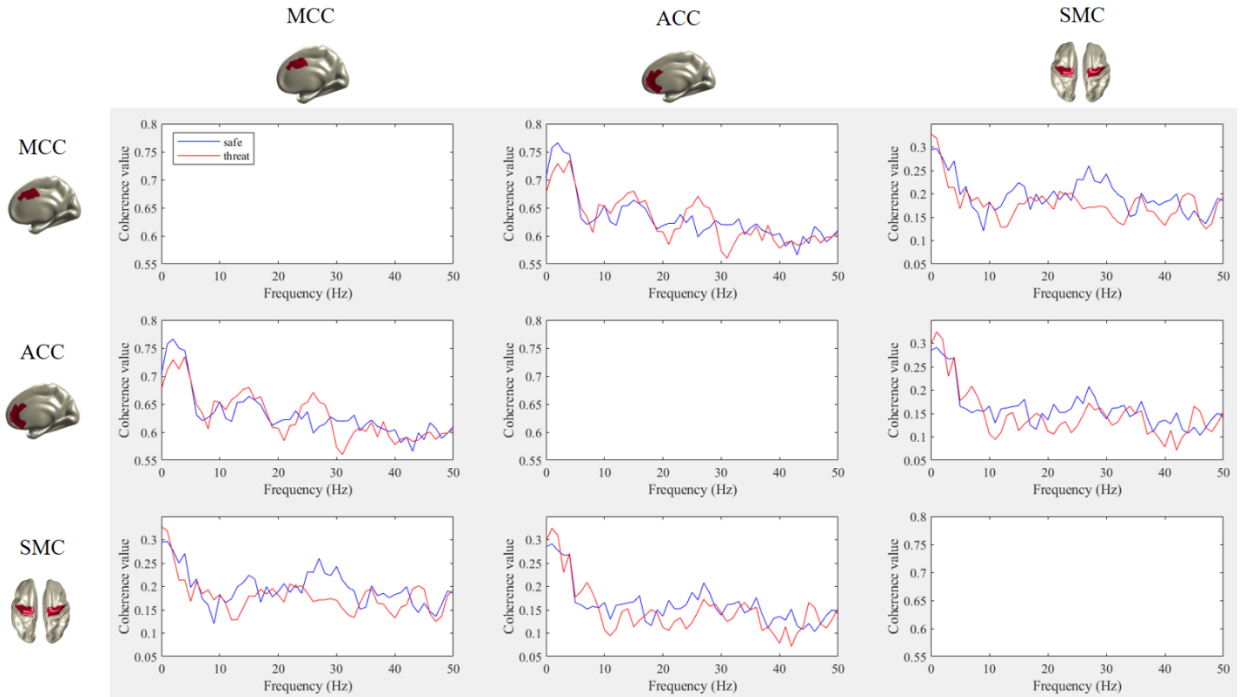

Figure S7: Coherence spectra during the switch to action - freeze only.

Coherence spectra were computed only for participants who showed threat-related bradycardia. Threat (red) and safe (blue) trials are compared during the switch to action.

Granger causality – freeze only: threat shoot versus safe shoot (switch to action)
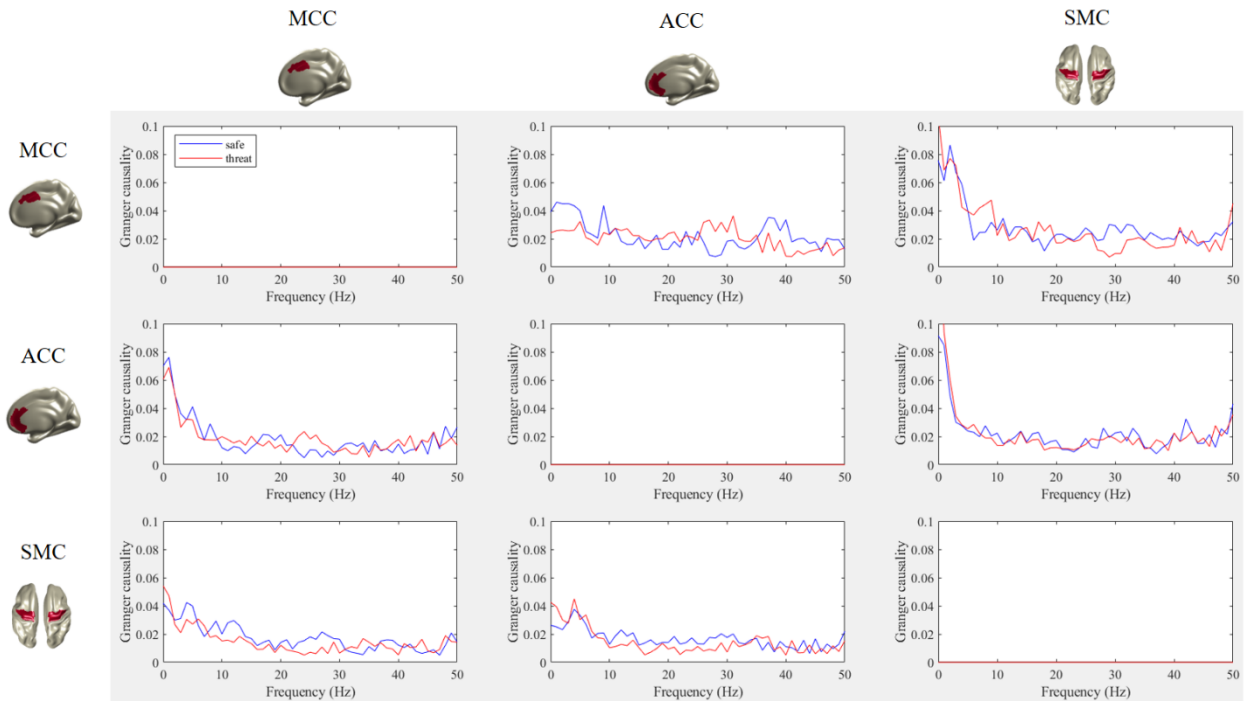

Figure S8: Granger causality spectra during the switch to action - freeze only.

Granger causality was calculated during the switch to action, and threat (red) and safe (blue) trials were compared.